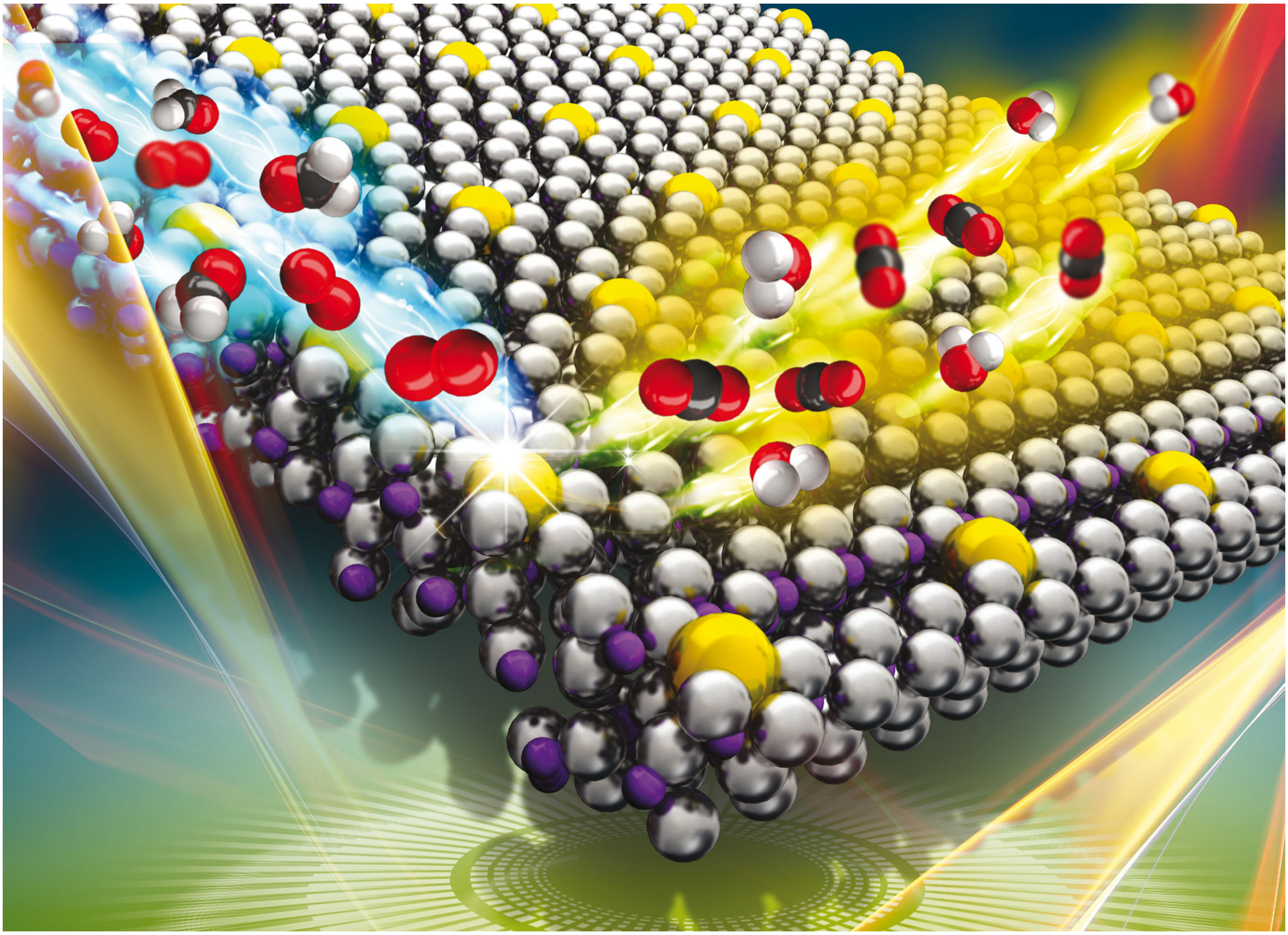

Showcasing research from Xingfu Tang's Laboratory, Department of Environmental Science and Engineering, Fudan University, Shanghai, China.

The active sites of supported silver particle catalysts in formaldehyde oxidation

Surface silver atoms with upshifted d-orbitals are identified as the catalytically active sites of formaldehyde oxidation by correlating activity with the number of the surface silver atoms, and the degree of the d-orbital upshift governs catalytic performance of the active sites.

As featured in:

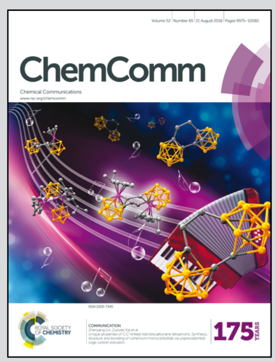

See Xingfu Tang *et al.*, *Chem. Commun.*, 2016, **52**, 9996.

ROYAL SOCIETY OF CHEMISTRY

www.rsc.org/chemcomm

Registered charity number: 207890

ChemComm

COMMUNICATION

View Article Online
View Journal | View Issue

Cite this: *Chem. Commun.*, 2016, 52, 9996

Received 13th April 2016, Accepted 30th June 2016

DOI: 10.1039/c6cc03097a

www.rsc.org/chemcomm

The active sites of supported silver particle catalysts in formaldehyde oxidation†

Yaxin Chen, Zhiwei Huang, Meijuan Zhou, Pingping Hu, Chengtian Du, Lingdong Kong, Jianmin Chen and Xingfu Tang*

Surface silver atoms with upshifted d-orbitals are identified as the catalytically active sites in formaldehyde oxidation by correlating their activity with the number of surface silver atoms, and the degree of the d-orbital upshift governs the catalytic performance of the active sites.

Precise identification of catalytically active sites (CASs) and a clear understanding of the intrinsic nature of the CASs are key requirements in heterogeneous catalysis, but remain challenging. Since the notion of the CASs was introduced by Taylor in 1925,[1] great efforts have been made in identifying the CASs, which is one of the fundamental prerequisites for fully understanding the intrinsic nature of the CASs, in order to improve the existing catalysts or design superior new catalysts.[2–4] However, the precise identification of the CASs is extremely difficult, especially for supported metal nanoparticle (NP) catalysts, due to their structural complexity. Fujitani *et al.* found that the CASs of Au/TiO_2 for CO oxidation were temperature-dependent and at low reaction temperatures the CASs were located only at the perimeter interfaces of the Au NPs in contact with the TiO_2 support and at high temperatures all the surface Au atoms acted as the CASs.[5] Typically, Ertl's group reported that the active metal surfaces often oscillate during the real catalytic oxidation,[6] meaning that the CASs are changeable. Therefore, it is a formidable task to identify the CASs of supported metal NP catalysts, which is also associated with a correct understanding of the intrinsic nature of the CASs.

To investigate the nature of the CASs, one often designs a series of catalysts by depositing different kinds of metal NPs onto the surface of a single support. Acerbi *et al.* intensively studied metal–CeO_2 catalysts and correlated the d-band centroids of different metals that were introduced by Nørskov *et al.*[7] with catalytic performance.[8] Although such a d-band centroid is an exciting electronic descriptor for the CASs, it ignores the effects of the kinds of metals on the catalytic performance (putatively called "metal effects"). In fact, low-temperature catalytic oxidation occurring over metal NPs supported on reducible oxides often follows a metal-assisted Mars–van-Krevelen mechanism,[9] so the kinds and structures of supports also have important influences on the electronic features of the CASs (tentatively called "support effects"). We recently supported silver (Ag) atoms on the surfaces of hollandite manganese oxides (HMO) with different structures,[10] and found that the surface Ag atoms also had different electronic states that could be described by a so-called d-orbital centroid (ε_{orb}), thus leading to different catalytic performances.[9] However, such metal/support effects should be ruled out for a clear understanding of the intrinsic nature of the CASs. Hence, a design by supporting the same kind of metals on the same supports is favourable for this purpose.

Herein we design a series of catalysts by supporting Ag NPs with different sizes on the same HMO support to study the intrinsic nature of the CASs in catalytic oxidation. Firstly, we synthesize a series of supported Ag catalysts and determine the average sizes of Ag NPs by various characterisation techniques. Next, we identify the CASs in the complete oxidation of formaldehyde (HCHO) at low temperatures, because HCHO is a typical air pollutant,[11,12] which greatly contributes to atmospheric particulate emissions.[13] Finally, we study the electronic structure of the surface Ag atoms to understand the intrinsic nature of the CASs, and establish the relationship between the electronic states of the CASs and the catalytic activity.

To synthesize a series of supported Ag catalysts with different sizes, we firstly supported truncated Ag octahedral NPs ~2 nm in height and ~4 nm in width on the HMO surfaces to get a Ag_{NP}/HMO sample, as shown in the HRTEM image and the model of Fig. S1 (ESI†). As evidenced in our recent work,[14] the sizes of Ag NPs could be readily controlled by using different annealing temperatures. Fig. 1 shows the HRTEM images of the Ag_{NP}/HMO sample heated by an electron beam. The Ag octahedra with different sizes on the HMO surfaces are clearly observed in Fig. 1a and b, and ultimately the atomically dispersed Ag catalyst was obtained, as shown in Fig. 1c.[14] Similarly, the sizes of the

Institute of Atmospheric Sciences, Shanghai Key Laboratory of Atmospheric Particle Pollution and Prevention (LAP[3]), Department of Environmental Science and Engineering, Fudan University, 220 Handan Road, Shanghai 200433, China. E-mail: tangxf@fudan.edu.cn

† Electronic supplementary information (ESI) available. See DOI: 10.1039/c6cc03097a

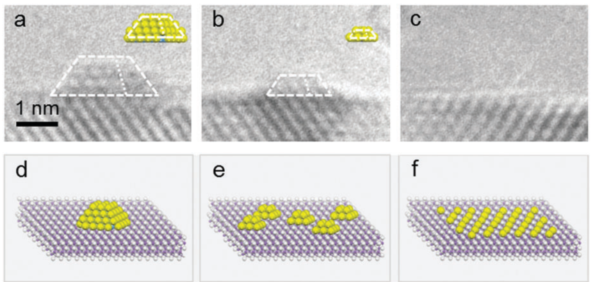

Fig. 1 (a–c) The shrinking process of the supported Ag NPs heated by an electron beam. Insets: The corresponding truncated Ag octahedra in (a and b). (d–f) Model illustrations of the synthesis process of the supported Ag catalysts with different metal sizes. Yellow, blue, grey and purple balls represent surface Ag, bulk Ag, O and Mn atoms, respectively.

Ag NPs could also be controlled by heating Ag_{NP}/HMO in air at different temperatures, as shown in synchrotron X-ray diffraction (SXRD) patterns of Fig. 2a. Thus, three supported Ag catalysts were synthesized by annealing the Ag_{NP}/HMO sample at different temperatures, 150, 200, and 350 °C, and are denoted as Ag_{82}/HMO, Ag_{13}/HMO and Ag_1/HMO, respectively. The number in the subscript represents the average number of Ag atoms in each Ag NP according to the following extended X-ray absorption fine structure (EXAFS) spectra in Fig. 2b. For example, "13" in Ag_{13}/HMO represents that each Ag NP consists of 13 Ag atoms in this catalyst. The shapes of the three catalysts were modelled as shown in Fig. 1d–f, according to the HRTEM images.

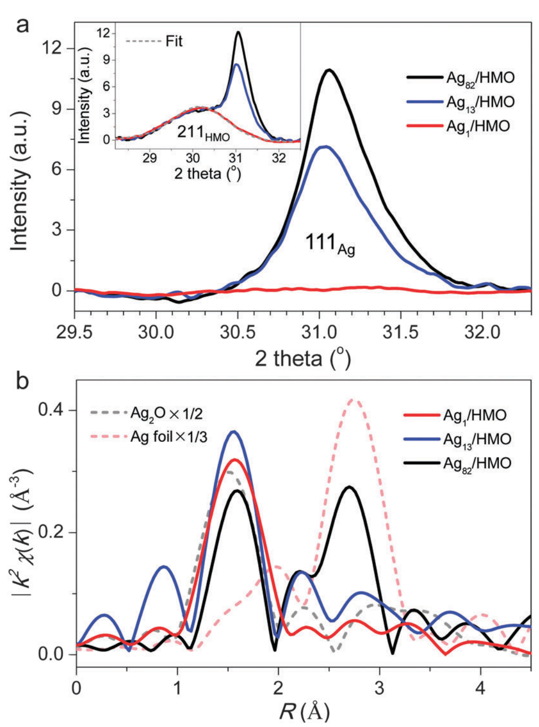

Fig. 2 (a) The Ag(111) diffraction peaks in the SXRD patterns of the three supported Ag catalysts obtained by subtracting the HMO(211) diffraction peaks from the original SXRD patterns (inset). (b) $\chi(R)$ k^2-weighted FT EXAFS spectra of the three supported Ag catalysts, the Ag foil, and Ag_2O.

Fig. 2b shows the Fourier transform (FT) amplitudes of the $\chi(R)$ k^2-weighted EXAFS data at the Ag K-edge of the three catalysts. The structural parameters obtained by fitting the spectra with theoretical models are summarized in Table S1 (ESI†).[15] The curve-fitting of the *R*-space, and the inverse FT spectra are given in Fig. S2 and S3 (ESI†). The nearest neighbour Ag–Ag coordination shell appears in the FT spectrum of Ag_{82}/HMO with an average distance of ~2.87 Å and a coordination number (CN) of ~8.0. According to the relationship of the CN to the size of metal NPs[16] (Fig. S4, ESI†), the average size of the Ag NPs in the Ag_{82}/HMO sample was estimated to be ~1.6 nm, on the basis of which the number of Ag atoms in each Ag NP was readily calculated to be 82 by considering the truncated Ag octahedral morphology of the Ag NPs (Fig. 1a and d). Similarly, a CN of ~2.6 was estimated according to the FT EXAFS spectrum of Ag_{13}/HMO (Fig. 2b and Fig. S2, S3, Table S2, ESI†), corresponding to the Ag NPs with an average size of 0.6 nm which consisted of 13 Ag atoms (Fig. 1b and e). For Ag_1/HMO after annealing at 350 °C, the FT amplitude in 2.7–3.0 Å was absent, indicating the formation of isolated Ag atoms.[14,17] The first shell in the FT spectrum of Ag_1/HMO with a distance of ~2.33 Å was assigned to the Ag–O bonds with a CN of 4, indicating the isolated Ag atoms were anchored onto the HMO surfaces.[14] Hence, a series of catalysts with different metal sizes were successfully synthesized by controlling the annealing temperatures.

Without the metal effects and the support effects, it is convenient for us to study the intrinsic nature of the CASs of the series of catalysts, but one of the important prerequisites is to clearly identify the CASs in catalytic reactions. However, accurate identification of the CASs remains challenging especially for supported metal particle/cluster catalysts due to the quantum size effect[18–20] and the structure-sensitive geometric effect.[21,22] Metal atoms at different local environments such as at steps, edges, kinks and corners often have different electronic states,[22] thus exhibiting different catalytic reactivities. Occasionally, it is controversial to identify the CASs of supported metal particle/cluster catalysts even under similar experimental conditions such as the same reactions and the same catalysts.[5,23] Alternatively, Cargnello *et al.* provided a robust method to identify the CASs of supported metal particle/cluster catalysts by establishing a model and correlating the fraction of atoms located at various surface sites with the turnover frequency (TOF) in CO oxidation over supported metal NP catalysts with different sizes.[24]

We followed Cargnello's method to determine which part of surface Ag atoms are the CASs in the complete oxidation of HCHO.[24,25] We first evaluated the catalytic performance of the three catalysts by studying the reaction kinetics in the HCHO oxidation at low temperatures, where the HCHO conversions were controlled to be lower than 20% (Fig. S5, ESI†), and then used Cargnello's method to identify the CASs. The results are reported as kinetic plots in Fig. 3a. The supported Ag catalysts drastically enhanced the catalytic activity in comparison to the pure HMO support, which was not active in the HCHO oxidation under the identical reaction conditions (Fig. S6, ESI†), indicating that the CASs were located on the surfaces of the Ag NPs, and especially for the Ag_1/HMO catalyst where the surface isolated Ag atoms were the CASs. Although the three catalysts gave

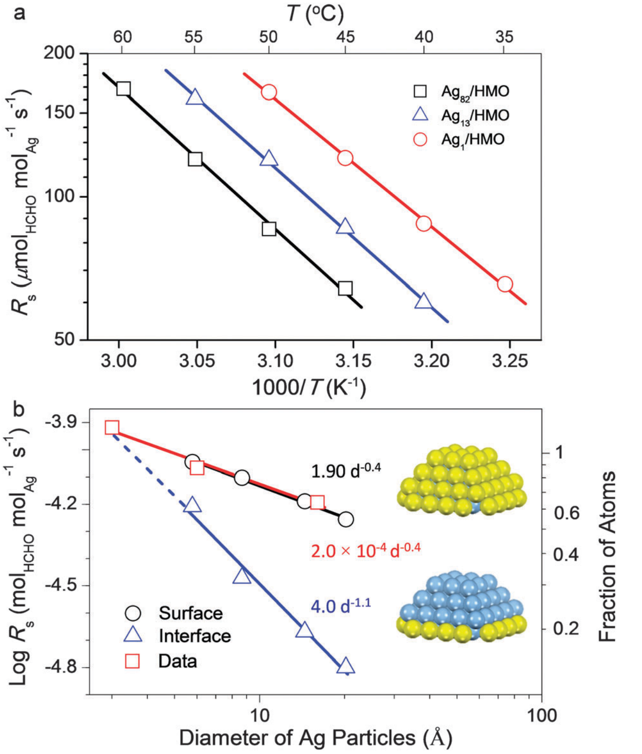

Fig. 3 (a) Arrhenius plots for the reaction rates (R_s) in the HCHO oxidation on the three supported Ag catalysts at low temperatures (T). (b) Calculated number of sites with a truncated Ag octahedral geometry (surface or perimeter atoms in contact with the support) as a function of diameter (d) and R_s at 45 °C of the three catalysts.

different reaction rates (R_s) in the HCHO oxidation, and the highest rate was achieved on the Ag_1/HMO catalyst, it is still difficult to find out where the CASs were located especially for Ag_{13}/HMO and Ag_{82}/HMO.

As a consequence, we calculated the fraction of atoms located at the various surface sites, and then plotted the fraction of atoms at a particular position as a function of particle diameter (d) for the models with different sizes (Fig. 3b).[25] These results showed a scaling of $d^{-0.4}$ or $d^{-1.1}$ for all the surface atoms or the Ag atoms at the perimeter of the Ag NPs in contact with the HMO support, respectively. We also calculated R_s over the three catalysts at 45 °C, and plotted the data on the same graph. Obviously, the reaction rates showed dependence on the diameter ($d^{-0.4}$). Therefore, this result clearly evidenced that all the surface Ag atoms of the Ag particles functioned as the CASs in the HCHO oxidation.[26] Although this result is different from Cargnello's result in that only the metal atoms in the periphery of metal NPs in contact with the supports acted as the CASs,[24] the proposed method is still valid in our catalytic systems, on the basis of which we calculated the TOFs of the three catalysts and found that the TOFs of both Ag_{13}/HMO and Ag_{82}/HMO were almost the same, but lower than that of Ag_1/HMO (Fig. S7, ESI†). Interestingly, the apparent activation energies (E_a) for two Ag NP catalysts, Ag_{82}/HMO (57 kJ mol^{-1}) and Ag_{13}/HMO (56 kJ mol^{-1}), were almost the same, which were higher than that (51 kJ mol^{-1}) for Ag_1/HMO (Fig. S6, ESI†), implying that their CASs had different electronic structures.

Owing to the almost same E_a of Ag_{13}/HMO and Ag_{82}/HMO in the HCHO oxidation, we comparatively studied the Ag electronic states of Ag_{13}/HMO and Ag_1/HMO by using the X-ray absorption near edge structure (XANES) spectra. Fig. S8 (ESI†) shows the Ag K-edge XANES spectra as a function of absorption energy for Ag_{13}/HMO and Ag_1/HMO together with two references, Ag_2O and Ag foil (ESI†). The white-lines of Ag_{13}/HMO and Ag_1/HMO were more intense than those of the two references, demonstrating that the electronic states of the two supported Ag catalysts were distinct from those of the Ag foil and Ag_2O.[14] The edge positions for Ag_{13}/HMO and Ag_1/HMO approached that of the Ag foil, indicating the Ag metallic states of the supported Ag catalysts. Subtly, the white-line feature of Ag_1/HMO was also different from that of Ag_{13}/HMO, reflecting the presence of the different electronic states of their CASs.

Density function theoretical calculations were carried out to confirm the electronic states of the CASs of Ag_1/HMO and Ag_{13}/HMO. According to the structures and morphologies of Ag NPs and HMO (Fig. 1 and Fig. S1, ESI†), we placed a truncated Ag octahedron consisting of 13 atoms and an individual Ag atom on the (110) surfaces of HMO as two models to investigate the electronic states of the CASs. The projected density of states (DOS) of the Ag d-orbitals was calculated and is shown in Fig. 4. The DOS of the surface isolated Ag atoms as the CASs of Ag_1/HMO was remarkably different from the Ag bulk, and the ε_{orb} of Ag_1/HMO was ~2.6 eV, upshifted by ~1.7 eV to the Fermi level compared with the Ag bulk (the d-band centroid of the Ag bulk is 4.3 eV).[27] For Ag_{13}/HMO, the DOS of 12 Ag atoms acting as the CASs is also displayed in Fig. 4. The average ε_{orb} of each Ag atom was ~3.7 eV, upshifted by ~0.6 eV with respect to the Ag bulk. Thus, the Ag atoms of the CASs for the series of catalysts had common electronic characteristics of the upshifted d-orbitals, which should facilitate the activation of the reactants, especially for molecular oxygen (O_2),[9,28] in the HCHO oxidation, and the degree of the upshift was also associated with E_a and catalytic activity.

Activation of O_2 was often considered as one of the important rate-limiting steps in catalytic oxidation,[17,29] which was closely associated with the electronic states or the ε_{orb} of the CASs.

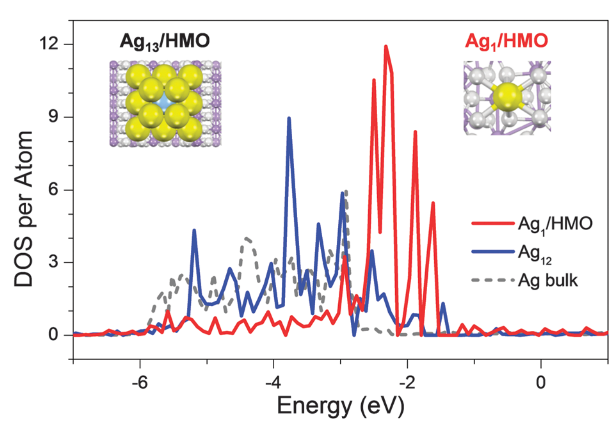

Fig. 4 Projected DOS of the Ag 4d orbitals of Ag_1/HMO, 12 surface Ag atoms of Ag_{13}/HMO (Ag_{12}). Insets: Two models of Ag_{13}/HMO and Ag_1/HMO. Yellow, blue, purple and grey balls represent surface Ag, bulk Ag, Mn and O atoms, respectively.

Nørskov *et al.* established a model to describe the relationship between the d-band centroid of the metal surfaces and the ability of the surface to bond to several adsorbates.[28] Mavrikakis *et al.* specialized Nørskov's model to a Ag–O system, and found that the upshifted d-band centroid of Ag facilitated the activation of O_2 by strong interaction of the Ag upshifted d-band centroid with a high-anti-bonding π^* orbital of O_2.[30] Paradoxically, the upshifted ε_{orb} of the CASs should be energetically favourable for dissociation of O_2 by charge transfer from the d orbitals of the active Ag atoms to anti-bonding π^* orbitals of O_2. Therefore, the intrinsic nature of the CASs could be described as the ε_{orb} upshift of the active Ag atoms in our catalyst system, and the degree of the upshift played a pivotal role in determining E_a in catalytic reactions such as HCHO oxidation and catalytic performance.[9,14]

In summary, we identified the CASs of the supported Ag particle catalyst in the HCHO oxidation, and studied the intrinsic nature of the CASs in catalytic oxidation by rationally designing a series of the supported Ag catalysts with different supported Ag particle sizes through elimination of the metal effects and the support effects. The combination of sophisticated characterisation techniques and reaction kinetics revealed that all the surface atoms of the Ag particles were the CASs. Theoretical calculations demonstrated that the active Ag atoms had the upshifted d-orbitals and the degree of the upshift was intimately related to the apparent activation energy and catalytic performance in the low-temperature oxidation. This provides a clear interpretation for the intrinsic nature of the CASs, which could assist the design of improved catalysts for low-temperature oxidation.

This work was financially supported by the NSFC (21277032 and 21477023) and the STCSM (14JC1400400). The X-ray absorption spectra and synchrotron XRD patterns were obtained at the Shanghai Synchrotron Radiation Facility.

Notes and references

1 H. S. Taylor, *Proc. R. Soc. London, Ser. A*, 1925, **108**, 105–111.
2 A. Bruix, J. A. Rodriguez, P. J. Ramirez, S. D. Senanayake, J. Evans, J. B. Park, D. Stacchiola, P. Liu, J. Hrbek and F. Illas, *J. Am. Chem. Soc.*, 2012, **134**, 8968–8974.
3 C. T. Campbell, *Nat. Chem.*, 2012, **4**, 597–598.
4 T. Zambelli, J. Wintterlin, J. Trost and G. Ertl, *Science*, 1996, **273**, 1688–1690.
5 T. Fujitani and I. Nakamura, *Angew. Chem., Int. Ed.*, 2011, **50**, 10144–10147.
6 R. Imbihl and G. Ertl, *Chem. Rev.*, 1995, **95**, 697–733.
7 A. Ruban, B. Hammer, P. Stoltze, H. L. Skriver and J. K. Nørskov, *J. Mol. Catal. A: Chem.*, 1997, **115**, 421–429.
8 N. Acerbi, S. C. Edman Tsang, G. Jones, S. Golunski and P. Collier, *Angew. Chem., Int. Ed.*, 2013, **52**, 7737–7741.
9 P. Hu, Z. Huang, Z. Amghouz, M. Makke, F. Xu, F. Kapteijn, A. Dikhtiarenko, Y. Chen, X. Gu and X. Tang, *Angew. Chem., Int. Ed.*, 2014, **53**, 3418–3421.
10 P. Hu, Z. Amghouz, Z. Huang, F. Xu, Y. Chen and X. Tang, *Environ. Sci. Technol.*, 2015, **49**, 2384–2390.
11 T. Salthammer, *Angew. Chem., Int. Ed.*, 2013, **52**, 3320–3327.
12 K. Toda, S. Yunoki, A. Yanaga, M. Takeuchi, S. I. Ohira and P. K. Dasgupta, *Environ. Sci. Technol.*, 2014, **48**, 6636–6643.
13 S. H. Jathar, T. D. Gordon, C. J. Hennigan, H. O. T. Pye, G. Pouliot, P. J. Adams, N. M. Donahue and A. L. Robinson, *Proc. Natl. Acad. Sci. U. S. A.*, 2014, **111**, 10473–10478.
14 Y. Chen, T. Kasama, Z. Huang, P. Hu, J. Chen, X. Liu and X. Tang, *Chem. – Eur. J.*, 2015, **21**, 17397–17402.
15 F. M. Chang and M. Jansen, *Angew. Chem., Int. Ed.*, 1984, **23**, 906–907.
16 E. Roduner, *Chem. Soc. Rev.*, 2006, **35**, 583–592.
17 Z. Huang, X. Gu, Q. Cao, P. Hu, J. Hao, J. Li and X. Tang, *Angew. Chem., Int. Ed.*, 2012, **51**, 4198–4203.
18 M. Valden, X. Lai and D. W. Goodman, *Science*, 1998, **281**, 1647–1650.
19 O. Lopez-Acevedo, K. A. Kacprzak, J. Akola and H. Häkkinen, *Nat. Chem.*, 2010, **2**, 329–334.
20 W. A. de Heer, *Rev. Mod. Phys.*, 1993, **65**, 611–676.
21 S. Dahl, A. Logadottir, R. C. Egeberg, J. H. Larsen, I. Chorkendorff, E. Törnqvist and J. K. Nørskov, *Phys. Rev. Lett.*, 1999, **83**, 1814–1817.
22 J. K. Nørskov, T. Bligaard, B. Hvolbæk, F. Abild-Pedersen, I. Chorkendorff and C. H. Christensen, *Chem. Soc. Rev.*, 2008, **37**, 2163–2171.
23 D. Widmann and R. J. Behm, *Angew. Chem., Int. Ed.*, 2011, **50**, 10241–10245.
24 M. Cargnello, V. V. T. Doan-Nguyen, T. R. Gordon, R. E. Diaz, E. A. Stach, R. J. Gorte, P. Fornasiero and C. B. Murray, *Science*, 2013, **341**, 771–773.
25 M. Shekhar, J. Wang, W. Lee, W. D. Williams, S. M. Kim, E. A. Stach, J. T. Milliams, S. M. Kim, E. A. Stach, J. T. Miller, W. N. Delgass and F. H. Ribeiro, *J. Am. Chem. Soc.*, 2012, **134**, 4700–4708.
26 W. Li, C. Stampfl and M. Scheffler, *Phys. Rev. Lett.*, 2003, **90**, 256102.
27 W. Wei, Y. Dai, M. Guo, Y. Zhu and B. Huang, *J. Phys. Chem. C*, 2010, **114**, 10917–10921.
28 C. F. Mao and M. A. Vannice, *J. Catal.*, 1995, **154**, 230–244.
29 B. Hammer and J. K. Nørskov, *Adv. Catal.*, 2000, **45**, 71–129.
30 Y. Xu, J. Greeley and M. Mavrikakis, *J. Am. Chem. Soc.*, 2005, **127**, 12823–12827.